

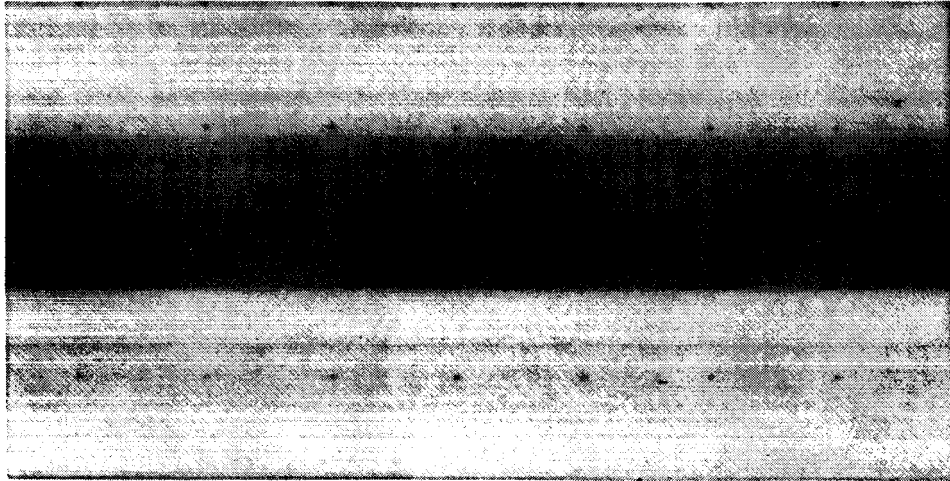
NAG 1-685

DAA / LANGLEY

1N-39

04836-CR

P.34



(NASA-CR-180679) POWER FLOW AS A COMPLEMENT
TO STATISTICAL ENERGY ANALYSIS AND FINITE
ELEMENT ANALYSIS Semiannual Report (Florida
Atlantic Univ.) 34 p Avail: NTIS HC
A03/MF A01

N87-26366

Unclas
0064836

CSSL 20K G3/39

FLORIDA ATLANTIC UNIVERSITY

College of Engineering • Department of Ocean Engineering

Center for Acoustics and Vibrations



POWER FLOW AS A COMPLEMENT
TO STATISTICAL ENERGY ANALYSIS
AND FINITE ELEMENT ANALYSIS

J.M. Cuschieri
Center for Acoustics and Vibration
Department of Ocean Engineering
Florida Atlantic University
Boca Raton, Florida 33431

February 1987

First Semi-Annual Report
Grant No. NAG-1-685

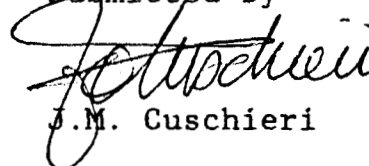
Submitted to
NATIONAL AERONAUTICS AND SPACE ADMINISTRATION
LANGLEY RESEARCH CENTER
HAMPTON, VA 23665

FORWARD

This report describes the work done at the Center for Acoustics and Vibration, in the Department of Ocean Engineering at Florida Atlantic University, under research grant number NAG-1-685. The work reported herein covers the period of research activities from September 1, 1986 to February 28, 1987.

The author wishes to acknowledge the assistance of Ms. M. McCollum, J.L. Rassineaux, and T. Gibert for their contribution in this research work.

Submitted by

A handwritten signature in dark ink, appearing to read 'J.M. Cuschieri', is written over the printed name.

J.M. Cuschieri

Principal Investigator

ABSTRACT

Power Flow as a Complement to Statistical Energy Analysis and Finite Element Analysis

Present methods of analysis of the structural response and the structure-borne transmission of vibrational energy use either finite element (F.E.) techniques or statistical energy analysis (SEA) methods. FE methods are a very useful tool at low frequencies where the number of resonances involved in the analysis is rather small. On the other hand SEA methods can predict with acceptable accuracy the response and energy transmission between coupled structures at relatively high frequencies where the structure modal density is high and a statistical approach is the appropriate solution. In the mid-frequency range, a relatively large number of resonances exist which make finite element methods too costly and possibly not feasible computationally. On the other hand SEA methods can only predict an average level from which significant deviations can occur at the resonances of the structure. In this mid-frequency range a possible alternative is to use power flow techniques, where the input and flow of vibrational energy to excited and coupled structural components can be expressed in terms of input and transfer mobilities. The type of mobility to be used depends on the type of excitation, moment or force and the type of junction, line, point or surface. This power flow technique can be

extended from low to high frequencies and this can be integrated with established finite element models at low frequencies and SEA models at high frequencies to form a verification of the method.

This method of structural analysis using power flow and mobility methods, and its integration with SEA and FE analysis is applied to the case of two thin beams joined together at right angles. The results show that indeed in the mid-frequency range the power flow method can be very useful since it can be used to estimate the structural response, including the high response near the resonances of the combined structure.

POWER FLOW
AS A COMPLEMENT TO SEA AND FINITE ELEMENT ANALYSIS

J.M. Cuschieri
Center for Acoustics and Vibration
Department of Ocean Engineering
Florida Atlantic University
Boca Raton, Florida, 33431

INTRODUCTION

In the analysis of the vibration response and structure-borne vibration transmission between elements of a complex structure, statistical energy analysis (SEA) or finite element analysis (FEA) methods are generally used. The choice is generally based on whether the required analysis is for low frequencies or high frequencies, which require the use of FEA and SEA respectively. SEA methods give relationships between spatial and spectral averages which are more than sufficient in high modal density regions. However these methods give only mean levels in regions of low modal density, and thus in these regions, the results obtained using SEA methods become unreliable. Large differences can occur between the actual structure behavior and the estimated behavior. One advantage of using SEA methods is that in some instances only the general geometrical characteristics of the structure are required and therefore generic structures can be investigated using the same model. In other instances this may be considered as a limitation on the method. If detailed analysis is required, in sufficiently low modal density regions, then FEA methods can be used. The implementation of FEA analysis is usually very time consuming, the modeling of the structure is very critical, especially as the frequency increases, and the number of modes that can be analyzed is usually limited. Thus while this method is very useful, in general the structure has to be accurately modelled and the

complete structure has to be analyzed which for very large complex structures can be costly and possibly not computationally feasible unless limited to only a few modes.

Therefore SEA and FEA methods, while both are extremely useful in their respective frequency regions, leave an empty gap in the mid-frequency range, where the modal density is not high enough for frequency averaging to give reliable results, but where a number of modes are present which can make FEA methods unwieldy. Secondly, because of their inherent characteristics, combining the two methods in the intermediate frequency regime is not straight forward. It is in these areas where the structural power flow techniques [1] are useful.

THE POWER FLOW METHOD

In using power flow methods, the structure is modeled by a series of coupled substructures, similar to SEA methods. Each substructure is analyzed independent of the other substructures with forces or moments separately introduced at all the junction locations with the other substructures. Associated with these joints' forces and moments are structural mobility functions. The input and flow of vibrational energy to and from the excited substructure to the other substructures is expressed in terms of input and transfer structural mobilities. The type of structural mobilities to be used at the different joints depends on the type and configuration of the joints. The form of the results for the response of the global structure will depend on the form of the structural mobility functions. Detailed response

of the global structure can be obtained if the narrow band frequency detail is retained in the structural mobility terms.

The mobility functions represent the response of the substructures. These response functions can be derived either in terms of mean response levels, or alternatively (usually at low and medium frequencies) the exact resonant response of the structure can be represented. The representation of mobility functions using mean response levels are in general independent of the exact structural geometries. The mean response level is only a function of the structure general characteristics. The low and medium frequency response, on the other hand is strongly dependent on the exact geometry of the structure. That is, at high frequencies where mean response levels can be used to give reliable results, the power flow method is identical to the SEA methods, and indeed the same results can be produced. This is a very useful feature because SEA methods are already well established and have proven to give reliable results at high frequencies. The fact that power flow methods can be frequency averaged at high frequencies to give the same results as SEA methods can be used as a verification tool to ensure that a reliable structural model is being used with the power flow techniques. The results at high frequencies are asymptotically equal to the results obtained with the SEA method. The low frequency results using the resonant structural mobility terms can be directly compared to results obtained using FEA methods.

Therefore, power flow results can be directly compared to SEA results at high frequencies and FEA results at low frequencies. Thus, these two established techniques can be used to verify the power flow models at the high and the low frequencies respectively. Once this is achieved, then the method can be used to obtain the mid-frequency range results where the other methods are either unreliable or too large to handle. The advantage of the power flow method is that, while detailed structural geometries are still required for the analysis, the structure is subdivided into smaller substructures which can be easier to handle. Thus no structure is too large or too complicated, since the analysis can be performed on the individual substructures. The size of the substructures is arbitrarily chosen to satisfy some maximum complexity criteria, but at the same time not creating an enormous number of substructures. The joint characteristics between the substructures are however retained so that the results apply to the global structure.

The power flow approach is to model the global structure by substructural components which are selected to be of the "right" level of complexity. Expressions are then derived for the power flowing between the substructures in terms of the mobilities of the substructures [2]. These expressions can be matrix expressions depending on the number of substructures that are joined together. The mobility functions in these expressions are evaluated, either in detailed resonant form or as mean levels to obtain the desired results for the global structure. Depending

on the complexity of the substructures and the number of substructures used to model the whole structure, it may be possible to evaluate the structural mobility functions using analytical solutions for the response of the substructure. The analytical solutions may include such methods as closed form solutions of the equations of motion or other methods such as the use of displacement amplitude functions. Alternatively numerical methods, including FEA methods, can be used on the substructures to obtain the required structural mobility functions. This will still be more efficient than modelling the whole structure. Also, if the structure is available for testing then the structural mobilities for the substructural elements can be obtained experimentally. The fact that elements of the structure are tested separately can make experimental techniques very attractive since no special fixtures or supporting equipment will be required as would be the case, if the whole structure is tested.

The use of this power flow concept and its integration with FEA and SEA results are demonstrated in the following section where a simple coupled beam structure is investigated. The following example does not completely show the full potential of this technique because the structure chosen for the analysis is very simple structurally, however it does serve as a proof of principle. The advantage of selecting this simple structure is that a full analytical analysis can be performed.

L-SHAPED BEAM RESPONSE

Power flow methods are used to obtain the response of one side of an L-shaped beam when the other side is excited by a point force. The results for the transmitted power to the receiver beam are compared to calculated transmitted power levels using FEA and SEA methods. Also the results are compared to results obtained from the closed form solution to this particular structural problem. Because a simple beam structure is chosen for this proof of principle it was a simple matter to evaluate the exact response of the beam structure. The L-shaped beam configuration and loading are shown in Figure 1. The common response that was selected for comparison between the different methods used in the analysis is the transmitted power to the receiver beam (beam 2 in Figure 1) or the ratio of transmitted to input power. To further simplify the problem the following assumptions are made:

1. The beams are thin compared to the wavelength so that rotary inertia, shear and inplane forces can be neglected.
2. The joint between the two beams is assumed pinned, that is no motion is allowed in the x or y directions at the joint.
3. The load is a point force applied at the free end of beam 1.
4. The common joint between the two beams is a rigid joint that is the angle between the two beams is always 90° .

In what follows the details of the different methods of analysis are presented, with the power flow method presented last.

FINITE ELEMENT ANALYSIS

To obtain the results using this method, the L-shaped beam is modelled using nineteen, 2 node Euler-Bernoulli beam linearly elastic elements. The nodes are equally spaced except near the right angled joint and at the beam ends. The location of these nodes are shown in Figure 2. The two beams are held at right angle near the corner joint by a stiff brace and the joint is externally pinned allowing only rotation in the x-y plane at the joint. That is each beam is not allowed to move longitudinally at the joint. Since the motion was restricted to transverse vibrations, only bending modes were considered. The MARC finite element package [3] was used for the analysis. To be able to compare the results to experimental analysis, the beams were assumed to have the material properties of steel. The brace was made significantly stiffer and of a very light material. In this way the influence of the brace on the natural frequencies of the structure is minimal, while still maintaining a 90 degree angle between the two beam elements at the joint. The only reason for introducing this corner brace was to simplify the section on the closed form solution analysis of the beams. Since the brace was not massless, and had some finite dimensions it would be expected that some disagreement would be obtained at high frequencies.

The analysis performed was restricted to frequencies between 1 Hz and 1000 Hz. Initially the natural frequencies and mode shapes were calculated and these were compared to the results obtained using the closed form solution to the equation of motion. The agreement was very close and thus the mean spatial average response for the receiver beam was calculated with the L-shaped beam subjected to harmonic excitation. For the harmonic analysis the excitation was restricted to between 1 and 1000 Hz.

The mean spatial average response at each frequency was calculated by integrating the root mean square (rms) velocity response over the length of the receiver beam and then dividing by the length of the beam. Using this approximation, reasonably accurate results were obtained provided each beam bending wave length contained at least three beam nodes. Thus the accuracy of the results decreased with increasing frequency. The power received by the receiver beam per unit force was calculated from the spatial average response per unit force. Since the beam is not connected to any other structure except the source structure, the transmitted power to the receiver beam is equal to the power dissipated by the beam.

$$\frac{\Pi_{\text{trans}}}{\text{unit force}} = \frac{\Pi_{\text{diss}}}{\text{unit force}} = \eta \, 2\pi f \, \rho A L \frac{\langle |V(f)|^2 \rangle}{|F(f)|^2} \quad 1.$$

Here η is the loss factor, f is the frequency, ρ , A and L the density, cross-sectional area and length of the beam respectively and $\langle |V(f)|^2 \rangle / |F(f)|^2$ the spatial averaged response per unit input force.

Statistical Energy Analysis

The L-shaped beam structure is considered as two coupled substructures with power input to one substructure and the objective is to obtain an expression for the ratio of the power transmitted to the receiver substructure per unit input power. The beam model and the SEA model are shown in Figure 3. The typical SEA energy relationships for the beam structure are given by

$$E_{\text{input}_1} = E_{\text{diss}_1} + E_{12} \quad 2.$$

$$0 = E_{\text{diss}_2} + E_{21} \quad 3.$$

The power transmitted from one substructure to the other Π_{ij} ($i=1,2$, $j=1,2$) is given using the usual SEA notation [4].

$$\Pi_{ij} = \omega \eta_{ij} (\langle E_i \rangle - \langle E_j \rangle) \quad 4.$$

and

$$\Pi_{\text{diss}} = \omega \eta_i \langle E_i \rangle \quad 5.$$

where η_{ij} and η_i are the coupling loss factor and the internal structural loss factor respectively and E_i and E_j are the energy levels of substructures i and j respectively. ω is the angular frequency.

Thus the ratio of transmitted power (same as dissipated power by receiver) to the input power is given by,

$$\frac{\eta_2 \omega \langle E_2 \rangle}{\Pi_{\text{input}_1}} = \frac{\eta_2}{\frac{(\eta_1 + \eta_{12})(\eta_2 + \eta_{21})}{\eta_{21}} - \eta_{12}} \quad 6$$

The coupling loss factors η_{12} and η_{21} are related to the junction transmission coefficient τ_{12} [5] defined as the ratio of transmitted to incident energy by

$$\eta_{12} = \frac{2}{\pi} \left(\frac{L_{12}}{k_1 A_1} \right) \tau_{12} \quad 7.$$

Where L_{12} is the length of the junction, A_i the area of the beam and k_i the bending wave number.

$$\eta_{21} = \eta_{12} (\eta_1 / \eta_2) \quad 8.$$

Where η_i ($i=1,2$) are the modal densities which for a beam asymptote at high frequencies to

$$\eta_i = L_i k_i / (2\pi\omega) \quad 9.$$

Where L is the length of the beam. The transmission coefficient has been evaluated by solving the solution for the beam motion at the junction. The model shown in Figure 4 is used in the analysis, where w_i represents the transverse displacements of the beams. The inplane displacements and the transverse displacement in the Z -direction are assumed negligible and are therefore not included in the analysis due to the pinned support at the joint.

Using continuity for the moment and angular displacement at the junction and the conditions specified in the assumption, that is, zero displacement at the joint and a rigid joint between the two beam substructures, an expression for τ_{12} is obtained.

$$\tau_{12} = \frac{|a_2|^2 D_2 k_2^3}{D_1 k_1^3} \quad 10.$$

where from the boundary conditions

$$a_2 = \frac{-1 + j}{\left[\frac{D_2 k_2}{D_1 k_1} + 1 \right] \frac{k_2}{k_1}} \quad 11.$$

and D_1 is the bending stiffness $D = EI/[A(1-\nu^2)]$.

Thus

$$\eta_{12} = \frac{4}{\pi} \cdot \frac{L_{12}}{A_1} \cdot \frac{1}{\left[\frac{D_2 k_2}{D_1 k_1} + 1 \right]^2} \cdot \frac{D_2 k_2^2}{D_1 k_1^2} \quad 12.$$

Substituting in equation (6) for η_{12} and η_{21} using equations (12) and (8), an expression for the ratio of transmitted to input power is obtained. In this case as well, the dissipated power is used since the input power must equal to the dissipated power as the substructure has no other connection except to the source substructure.

CLOSED FORM SOLUTION

The structure that has been selected for the analysis is very simply structurally and thus it is possible to determine a closed form solution to the equations of motion of the structure. Using the coordinates as defined in Figure 4 and placing the same motion restrictions as in the previous analysis sections, a solution is sought for the transmitted power and the input power. The transmitted power is computed using both equation 1, that is by calculating the dissipated energy, and also from the product of the moment and the rate of change of the angular displacement at the joint. The solutions to the equations of motion are of the usual form [6] that is for the source beam (beam 1).

$$w_1(x) = A_1 \cosh(kx) + B_1 \sinh(kx) + C_1 \cos(kx) + D_1 \sin(kx) \quad 13.$$

and for the receiver beam (beam 2).

$$w_2(y) = A_2 \cosh(ky) + B_2 \sinh(ky) + C_2 \cos(ky) + D_2 \sin(ky) \quad 14.$$

A_i , B_i , C_i and D_i ($i=1,2$) are arbitrary constants which

depend on the boundary conditions. For the problem at hand these conditions are::

Beams pinned at (0,0); $w_1(0) = w_2(0) = 0$, 15(a,b).

complement slopes at the joint; $\frac{\partial w_1(0)}{\partial x} = - \frac{\partial w_2(0)}{\partial y}$, 16.
(angular displacement continuity)

same bending moment at joint (0,0); $\frac{\partial^2 w_1(0)}{\partial x^2} = \frac{\partial^2 w_2(0)}{\partial y^2}$, 17.
(bending moment continuity)

At the free end of the receiver beam both the shear force and the bending moment are zero.

$$\frac{\partial^3 w_2(L)}{\partial y^3} = \frac{\partial^2 w_2(L)}{\partial y^2} = 0 \quad 18(a,b)$$

At free end of the source beam, bending moment equal zero but shear force is equal to the excitation force

$$\frac{\partial^3 w_1(L)}{\partial x^3} = \frac{-F}{EI} \quad 19.$$

$$\frac{\partial^2 w_1(L)}{\partial x^2} = 0 \quad 20.$$

Using these boundary conditions, expressions for A_i , B_i , C_i and D_i ($i=1,2$) are derived.

The input power is then given by

$$\Pi_{\text{input}} = \text{Real} \left[F^* \cdot j\omega w_1(L) \right] \quad 21.$$

and the transmitted power using moment and angular velocity at the joint is

$$\Pi_{\text{trans}} = \text{Real} \left[\left(\frac{EI \partial^2 w_2(0)}{\partial y^2} \right)^* j\omega \left(\frac{\partial w_2(0)}{\partial y} \right) \right] \quad 22$$

where ()^{*} implies complex conjugate. In these expressions the modulus of elasticity E, is taken to be complex to include the structural damping.

The transmitted power using the spatial average surface velocity is evaluated from the expression

$$\Pi_{\text{trans}} = \eta(\rho AL) \frac{2\pi f}{L} \int_0^L |j\omega w_2(y)|^2 dy \quad 23.$$

These expressions are evaluated per unit force input at frequencies within the interval 1 to 1000 Hz.

Power Flow Analysis

The L-shaped beam structure is divided into 2 substructures, each beam being a substructure and analyzed on its own. The joint conditions are however retained from the global structure. This will ensure that the final results will apply for the global structure. The objective, as in the other methods of analysis

presented in the previous section, is to obtain expressions for the transmitted power to the receiver beam and also for the ratio of transmitted to input power. In structural mobility terms the transmitted and input power for two coupled substructures are given by [1].

$$\Pi_{\text{trans}} = \frac{|F(f)|^2}{2} \left| \frac{M_{12}}{M_2 + M_3} \right|^2 \text{Real} \{M_3\} \quad 24.$$

and

$$\Pi_{\text{input}} = \frac{|F(f)|^2}{2} \text{Real} \left\{ M_1 + \frac{M_{12} M_{21}}{M_2 + M_3} \right\} \quad 25.$$

where M_1 is the input mobility at the excitation location, M_{12} is the transfer mobility between the excitation location and the joint location, M_2 is the input mobility at the joint location for the source substructure and M_3 is the input mobility at the joint location for the receiver substructure. Each of these mobility functions can be evaluated for the substructures separately. Mobility functions can be defined for both translational and rotational motions and excitations, or combinations and the selection is a function of the type of joint. Thus for the L-shaped beam structure, only rotational motion is being assumed at the joint and the mobility terms that are associated with the joint location are either in terms of rotational displacement or applied torque. M_{12} represents the angular response at one end of the beam per unit applied transverse load at the other end and M_{21} represents the response at the free end of the substructure due to the

application of a Torque at the joint location. Because of reciprocity, these two mobility functions will be identical. M_2 and M_3 represent the angular response per unit torque at the joint location for the two substructures respectively. M_1 represents the response per unit force at the excitation location.

Each of these mobility functions can be evaluated by separately considering each substructure. Thus to find M_{12} a beam (shown in Figure 5(a) with a transverse point load applied at one end and pinned at the other end (to retain the same condition of zero displacement at the joint, set in the previous analysis) is considered. Then

$$\begin{aligned}
 M_{21} = M_{12} &= \frac{j\omega (\partial w(0)/\partial x)}{F} \\
 &= \frac{-j\omega}{EIk^3} \frac{(\sin(kL) + \sinh(kL))}{[\cosh(kL)\sin(kL) - \sinh(kL)\cos(kL)]} \quad 26.
 \end{aligned}$$

The same model can be used to find M_1 .

$$\begin{aligned}
 M_1 &= \frac{j\omega w(L)}{F} \\
 &= \frac{-j2\omega}{EIk^3} \frac{\sinh(kL)\sin(kL)}{[\cosh(kL)\sin(kL) - \sinh(kL)\cos(kL)]} \quad 27.
 \end{aligned}$$

For M_2 and M_3 (these are equal since the source and receiver structures are identical)—the beam shown in figure 5(b) is considered, where one end is free and the other end has an applied bending moment Γ and

$$M_1 = \frac{j\omega(\partial w(0)/\partial x)}{\Gamma}$$

$$= \frac{-j\omega}{EI k^3} \cdot \frac{1 + \cosh(kL)\cos(kL)}{[\cosh(kL)\sin(kL) - \sinh(kL)\cos(kL)]} \quad 28.$$

$i = 2$ and 3 , and E is a complex quantity to include structural damping. These expressions (equations 26, 27, 28) can be inserted in equations (24) and (25) to obtain the transmitted power and the input power.

In the example that is being considered here the mobility functions for each of the substructures can be evaluated using closed form solutions for each of the substructures. This may not always be possible but other techniques are available. The advantages of using this power flow method over other methods are discussed in the next section after the presentation of the results.

RESULTS AND CONCLUSIONS

The results from all the above methods of analysis are presented in Figures 6-9. The results obtained using the power flow method and the closed form solution to the global structure are exactly identical and therefore these are represented on separate figures. Figures (5) and (6) represent the results for

the transmitted power using the closed form solution and the power flow methods respectively. Although the results are exactly identical the number of computations required using the power flow method is much less compared to the closed form solution. In the example discussed here, using the closed form solution for the whole structure resulted in 8 unknown constants which can be evaluated from the boundary conditions. The evaluation procedure can be viewed as the operation of inverting an 8×8 complex square matrix, representing the 8 simultaneous equations derived from the boundary conditions. Using the power flow method the computations are reduced in number because now there are two separate sets of 4 unknown constants which when represented in matrix form, consists of two 4×4 matrices from the two sets of boundary conditions. Inverting two 4×4 matrices is much more efficient (lower number of computations) as compared to inverting an 8×8 matrix.

On the same curve as the results from the power flow analysis are represented the results from the FEA method (Figure 6). Using the FEA method and keeping the analysis within reasonable bounds it was not possible to evaluate the response of the structure at frequency spacing as close as those used in the power flow method. The frequency resolution used was of 1 Hz between 1 Hz and 10 Hz and of 10 Hz between 10 and 1000 Hz. With this in mind the agreement in the results is quite good. At high frequencies the disagreement is attributed to the imperfectness of the FE model including the introduction of the brace. Below the first natural frequency the disagreement is caused by the

definition of the loss factor. This result was checked using the closed form solution results, that is the transmitted power evaluated using equations (23) and (22) and the same discrepancy is obtained below the first natural frequency. Thus this discrepancy is not an error of the power flow method.

Figures 8 and 9 represent the results for the ratio of transmitted to input power. As expected the same result is obtained using the closed form solution method (figure 8) and the power flow method (figure 9). The two results are shown in separate figures. Together with the power flow results in Figure (9) the results using the SEA method are shown. As expected the details of the analysis are lost if the SEA method is used. Also, using the SEA method significant under or over estimates can result in the estimated power reaching a particular substructure. The variations in the results will increase if the structure has a low loss factor as one might expect. In the analysis a loss factor of 0.01 was assumed. The curves shown in Figure 9 asymptotically collapse together as the frequency increases.

The advantages of using the power flow method over other methods can be deduced from these results and from consideration of the computational efficiency. The power flow and the closed form solution results have already been compared. The power flow can give the same results as the closed form solution but it is computationally more efficient. Compared to the FEA results, if the same resolution in frequency was to be retained the power flow method is vastly more efficient computationally compared to

the FEA method. The SEA method is more efficient computationally than the power flow method. However it is unreliable at low frequencies where the fluctuations from the mean can be significant. As the frequency increases the power flow results asymptotically approach the SEA results. If instead of using the resonant response in the mobility functions, mean values for the mobilities are used [7], then the results obtained using the power flow are exactly identical to the SEA results and computationally they are the same. This can serve as a verification of the model in the power flow method, since SEA methods are already well established. This was not necessary here because of the simple type of structure considered.

In conclusion, the power flow method is shown here to be a very powerful method. Although only demonstrated for two simple substructures, it is a simple matter to extend to multiple substructures, with multiple joints. The results produced have clearly demonstrated the usefulness of the power flow method at mid frequencies where SEA methods can be unreliable and FEA methods are critical on the exact representation of the structure, while keeping the number of nodes within acceptable limits. By dividing the structure into substructures, it may be possible to use analytical techniques to evaluate the mobility terms. If numerical methods have to be used, such as FEA methods, the problem of exact representation of the structure can be reduced if not eliminated because of the smaller sized

substructures that have to be dealt with. Also the power flow method has most of the advantages of the SEA method but still produces the detailed resonant behavior of the structure.

Another advantage that can be extremely useful for large complex structures is that, since the global structure is divided into substructures with each substructure evaluated separately, if some modification is made on the structure, only the substructure containing the modification needs to be remodelled and reanalyzed. This also applies to the SEA method. However, if FEA methods are used a complete analysis of the whole structure is required for every modification.

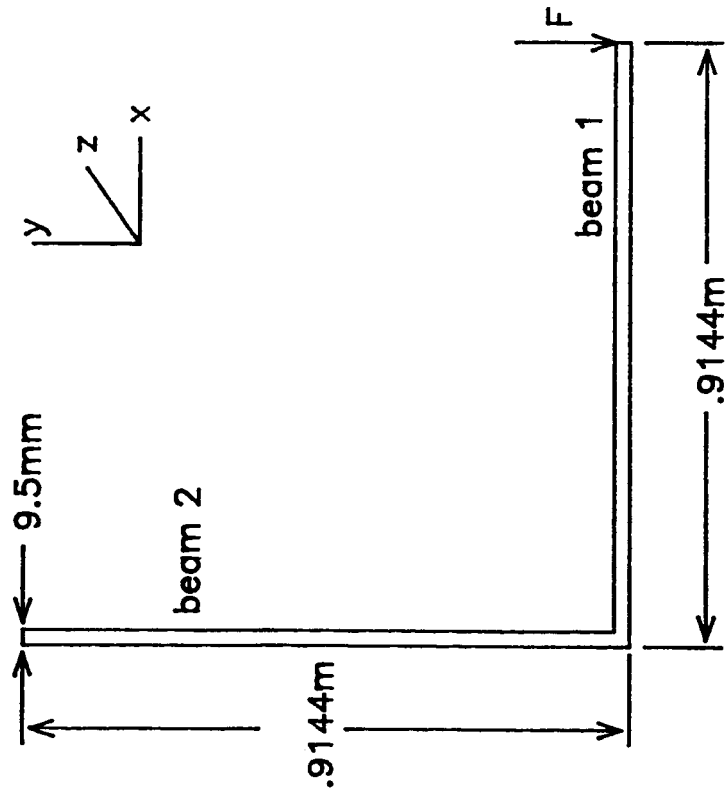
ACKNOWLEDGEMENT

The author would like to acknowledge the financial support by NASA under which this work was carried out. Also a special thanks to Ms. M. McCollum, Mr. J.L. Rassineux and Mr. T. Gibert who helped in the analysis that are presented in this paper.

REFERENCES

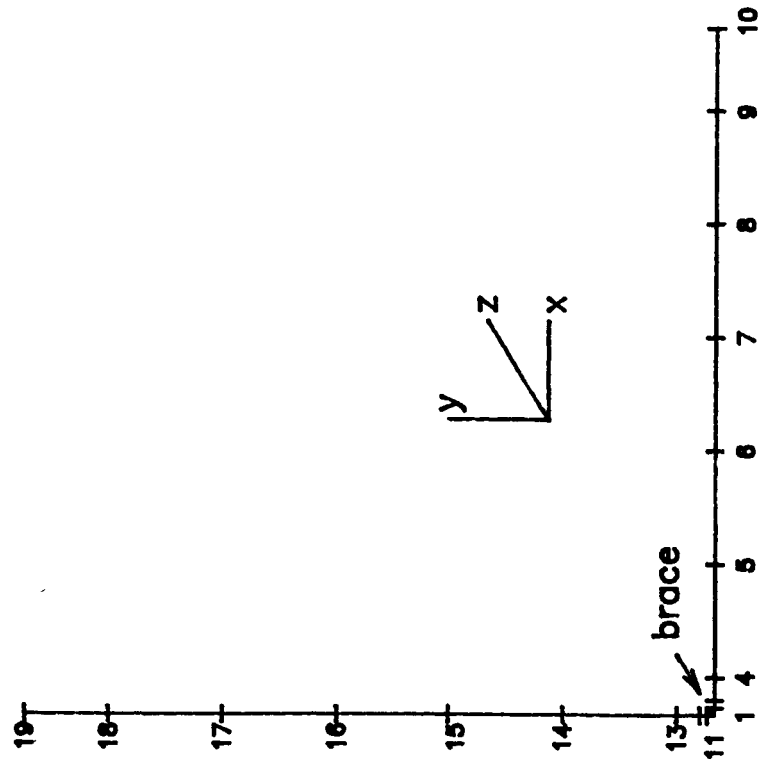
1. R.J. Pinnington, R.G. White (1981) Journal of Sound and vibration 75, 179-197, "Power Flow Through Machine Isolations to to Resonant and Non-resonant Beams".
2. J.W. Verheij, "Multipath Sound Transfer from Resiliently Mounted Shipboard Machinery", Institute of Applied Physics, FNO-TH, Delft, The Netherlands (1982).
3. "MARC General Purpose Finite Element Program", MARC Analysis Research Corporation, Palo Alto, California (1986 Edition).
4. R.H. Lyon and T.D. Scharton (1965) Journal of the Acoustical Society of America 38, 253-261, "Vibrational Energy Transmission in a Three Element Structure".

5. R.H. Lyon "Statistical Energy Analysis of Dynamic Systems"
MIT Press (1975).
6. E. Skudrzyk "Simple and Complex Vibratory Systems",
Pennsylvania State University Press (1968).
7. H.G.D. Goyder, R.G. White (198) Journal of Sound and
Vibration 68, 59-117, "Vibrational Power Flow from Machines
into Built-up Structures".



Material: Steel
 Density: 8000 Kg/m³
 Modulus of
 Elasticity: 200 GN/m²
 Loss Factor: 0.01

Figure 1. L-shaped beam structure.



Node	x	y	z
1	.00	.00	0.0
2	.01	.00	0.0
3	.03	.00	0.0
4	.05	.00	0.0
5	.20	.00	0.0
6	.35	.00	0.0
7	.50	.00	0.0
8	.65	.00	0.0
9	.80	.00	0.0
10	.91	.00	0.0
11	.00	.01	0.0
12	.00	.02	0.0
13	.00	.05	0.0
14	.00	.20	0.0
15	.00	.35	0.0
16	.00	.50	0.0
17	.00	.65	0.0
18	.00	.80	0.0
19	.00	.91	0.0

Figure 2. Finite element model showing node coordinates

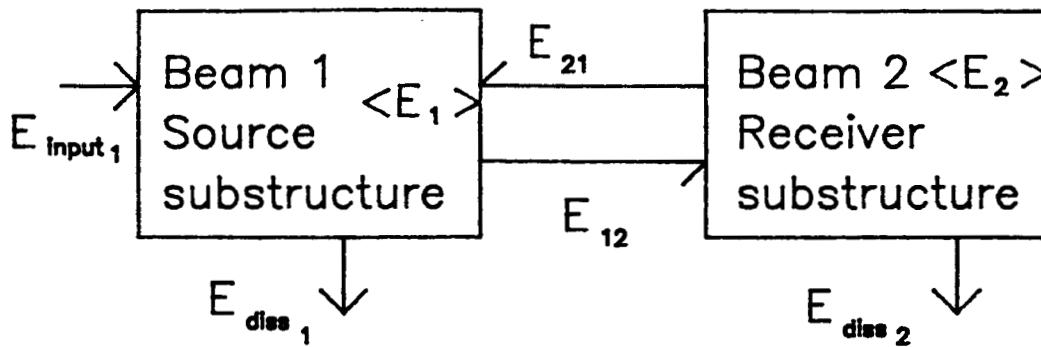


Figure 3. Statistical energy (SEA) model.

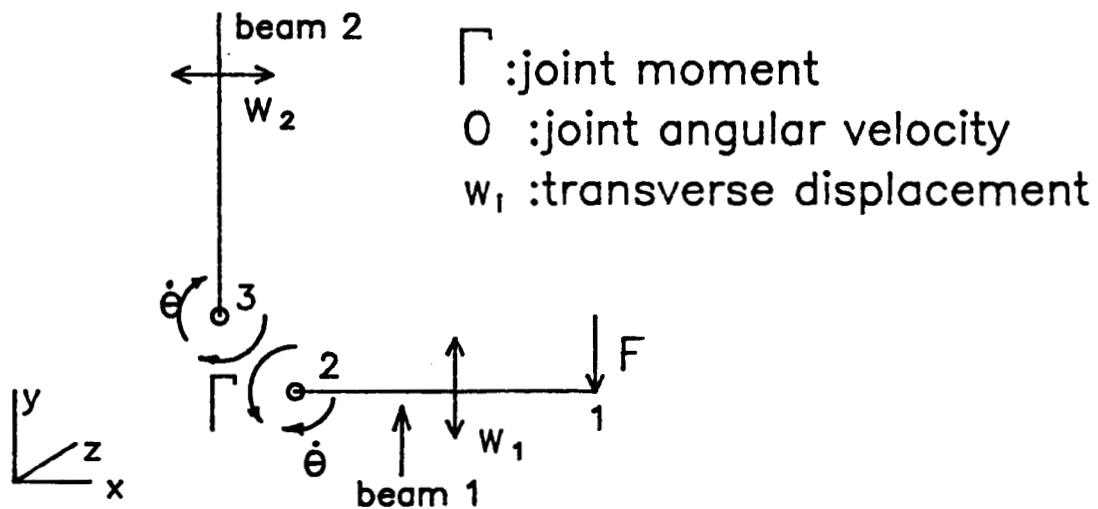


Figure 4. Beam joint constraints used in calculating τ_{12} and in the closed form solution.

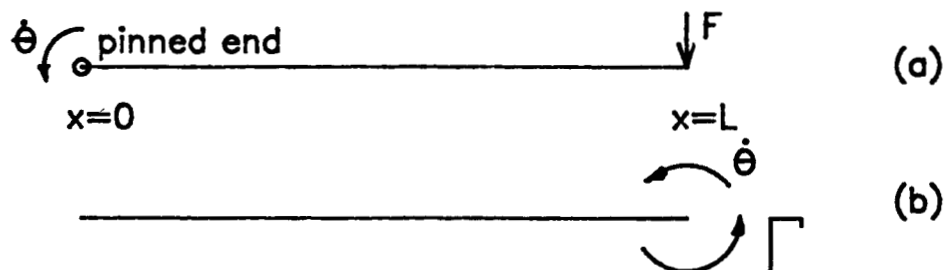


Figure 5. Substructural beam elements used in the power flow analysis. Note that joint conditions are retained so that the results can be used to obtain the response of the global structure.

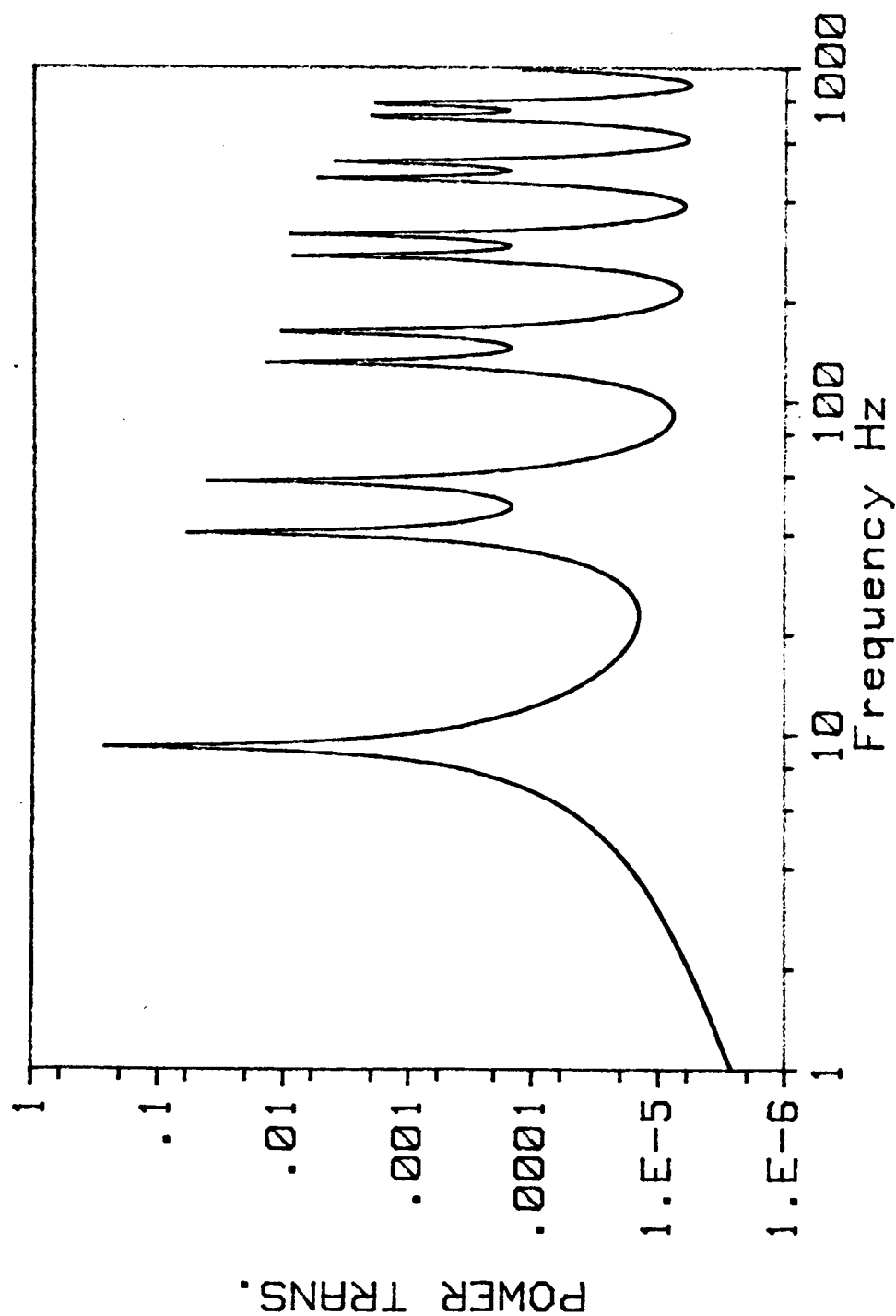


Figure 6. Power transferred to receiver beam using the closed form solution.

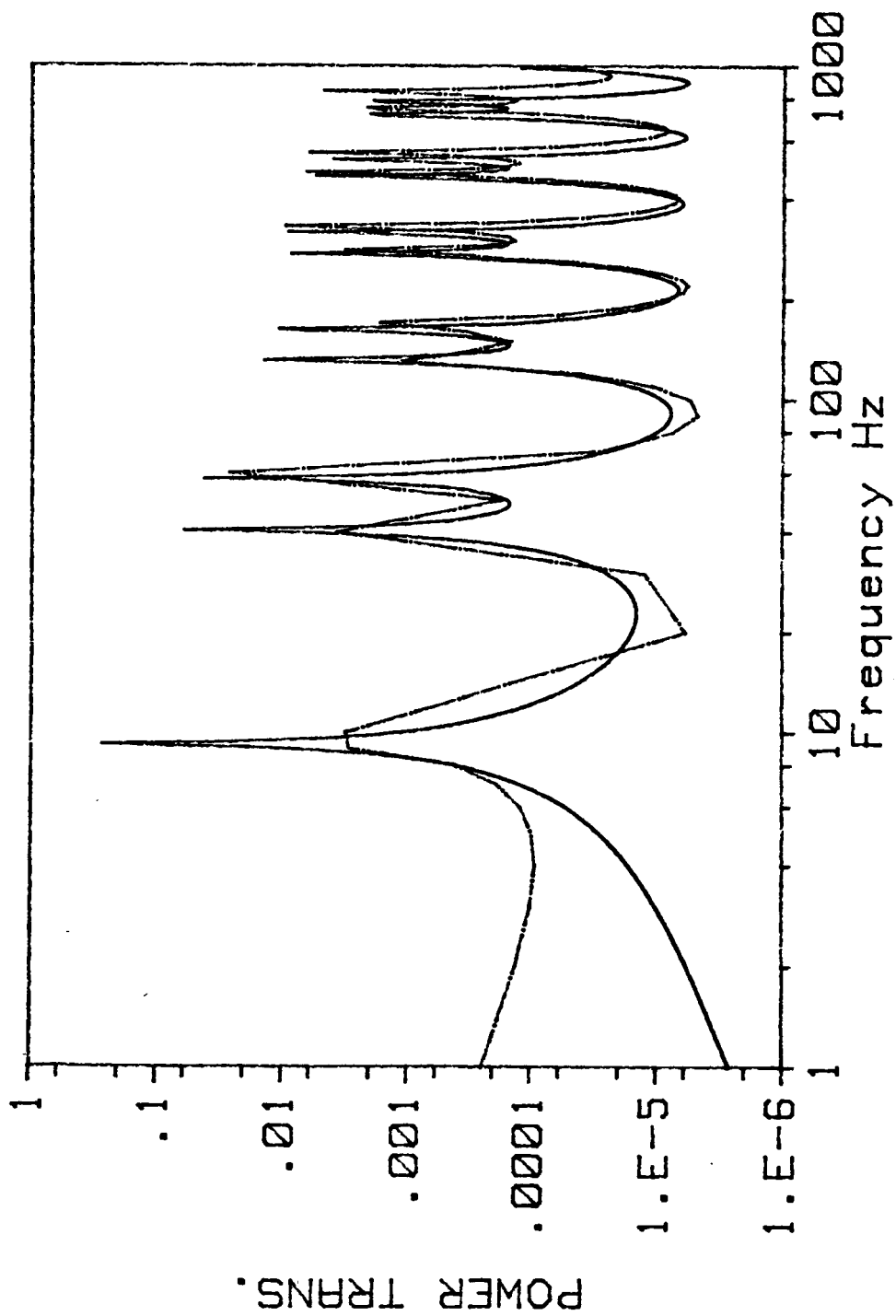


Figure 7. Power transferred to receiver beam using ____: power flow method; and _ _ _ _: finite element method.

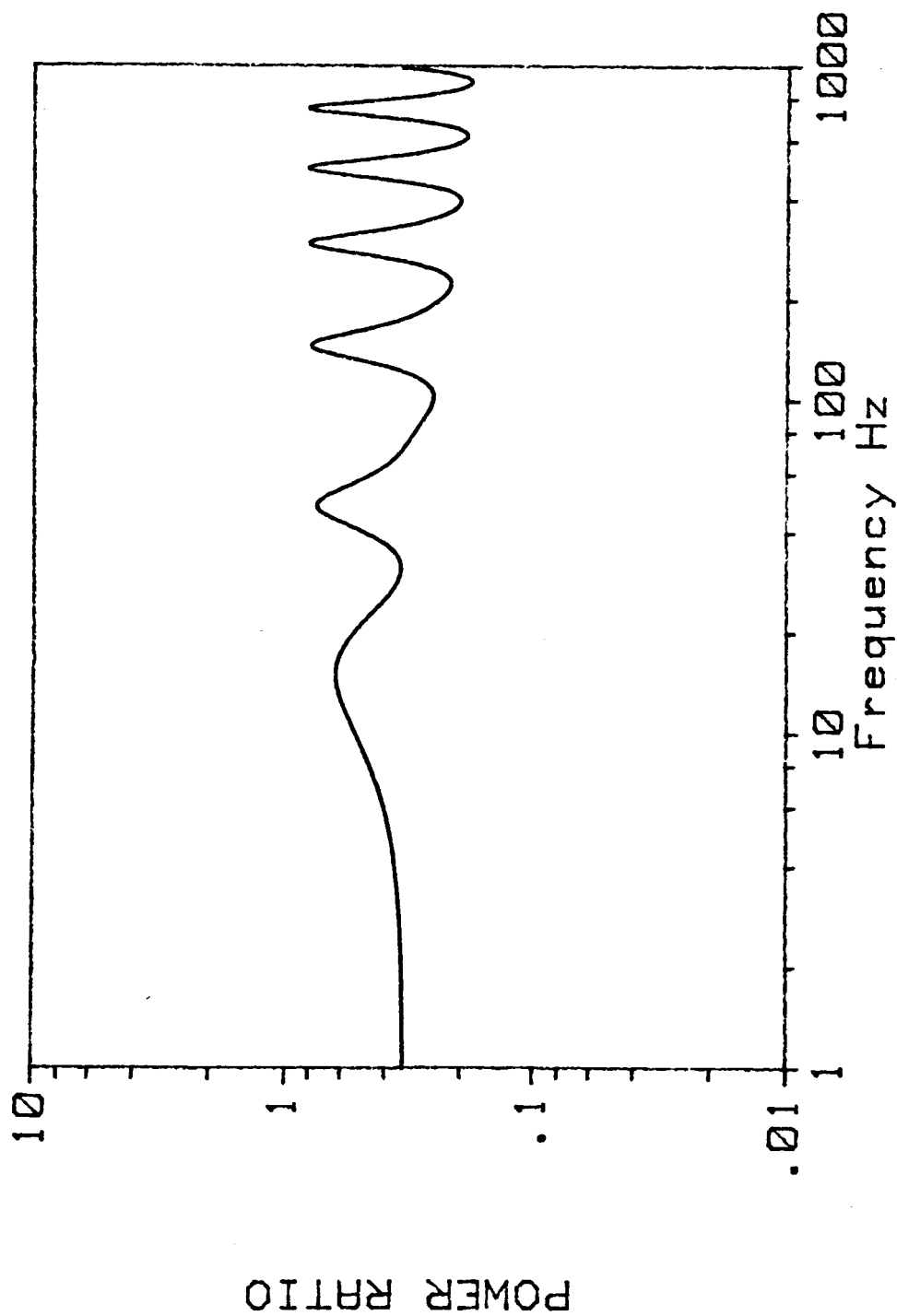


Figure 8. Ratio of transmitted to input power using the closed form solution.

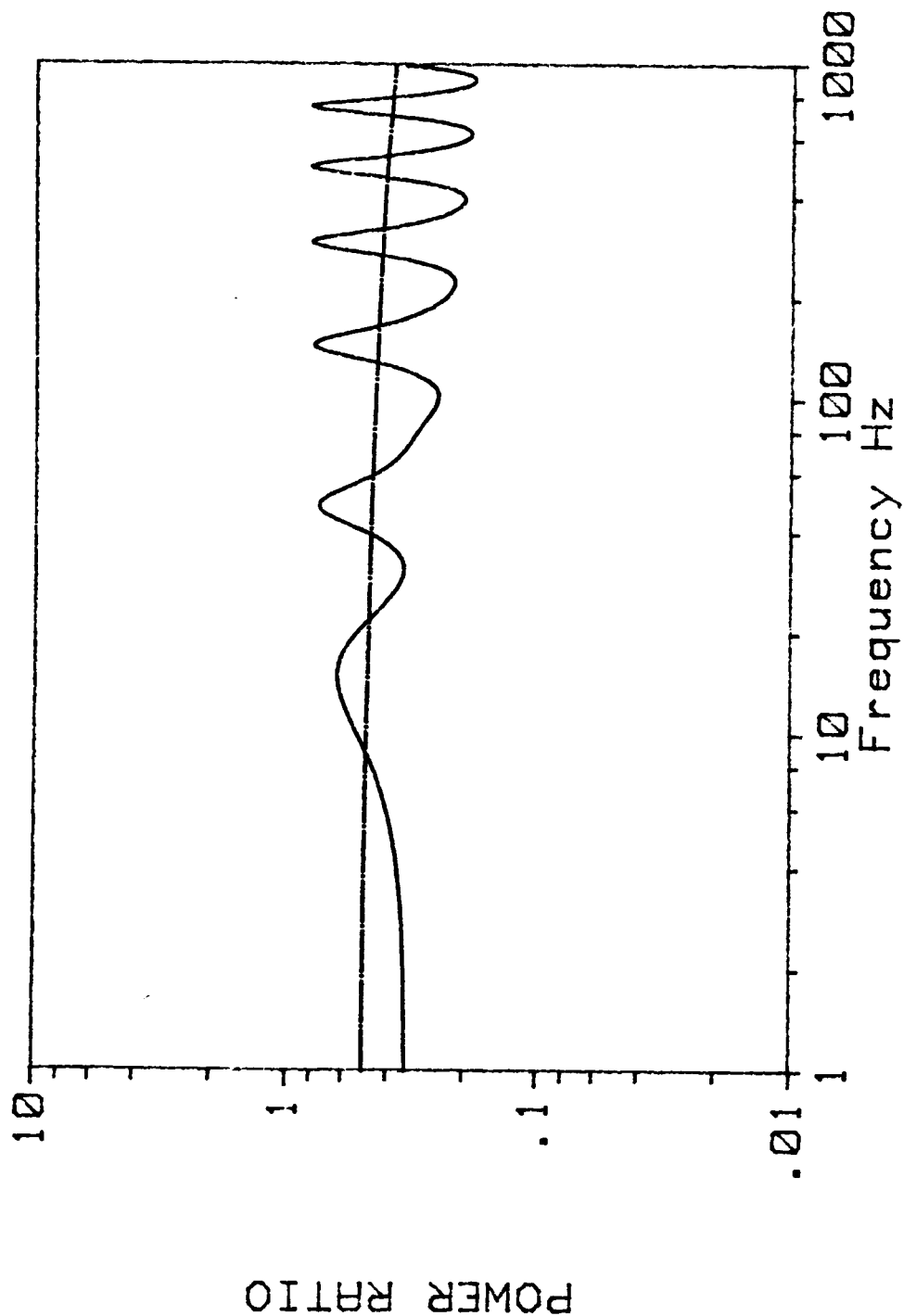


Figure 9. Ratio of transmitted to input power using ____: power flow method; -.-.: statistical energy method.